Supporting Information

Colossal Photodetection Enhancement via Plasmon-Exciton Synergy in Ultra-Smooth $CsPbBr_3$ Microplates

Zhaozhi Guan, Hua Mi,[a] Zairan Liu, Yan Tian, Haojian Lin, Huanjun Chen,* Shaozhi Deng* and Fei Liu*[c]

State Key Laboratory of Optoelectronic Materials and Technologies, Guangdong Province Key Laboratory of Display Material and Technology, and School of Electronics and Information Technology, Sun Yat-sen University, Guangzhou 510275, China

Corresponding Email: liufei@mail.sysu.edu.cn, chenhj8@mail.sysu.edu.cn, stsdsz@mail.sysu.edu.cn

1. The growth mechanism

The growth mechanism of our developed polydimethylsiloxane (PDMS)-assisted slow evaporation method should obey the classical theory of "Dissolution-Nucleation-Growth"[1] (Fig. R1). The growth process of the microplate can be depicted as follows. Firstly, the CsBr and $PbBr_2$ precursors will dissolve into polar organic solvents (DMF or DMSO). Secondly, the size of nucleus is dependent on the synergetic effect between the solute diffusion and surface reaction. When the stirring time is long enough over 24 hours, these two actions will arrive at the equilibrium, resulting in the formation of lots of $CsPbBr_3$ nuclei with uniform size based on the following reaction equation[2]:

$$PbBr_2 + CsBr \longrightarrow CsPbBr_3$$

Finally, with the progression of the low-temperature (>70 ℃) reaction, the nucleus gradually grows up and form monoclinic $CsPbBr_3$ microplates via the epitaxial growth on substrate[3]. Therefore, by controlling the solvent evaporation rate and the Van der Waals force between microplate and SiO_2 substrate, $CsPbBr_3$ microplates with atom-level smooth surface can be successfully fabricated in our work.

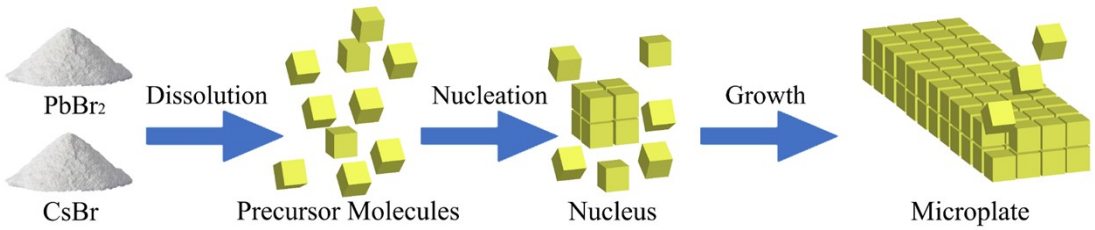

Fig. S1 The formation mechanism of $CsPbBr_3$ microplates.

2. The key factor on the growth of $CsPbBr_3$ microplates

Among all the experimental parameters, the solvent evaporation rate is the key factor determining the surface roughness of perovskite microplates in PDMS-assisted slow evaporation method, which can regulate the solute concentration in the reaction process[3].

Samples 1 and 2 respectively correspond to the growth substate without any weights and with a PDMS film during the evaporation process. And Samples 3 and 4 have a top weight of 13 g or 18.1 g, respectively. Through modulating the mass of top weight, we can obtain different solvent evaporation rates (60, 15, 7.5 and 3.6 μL/h), as shown in Fig. R2(a-d). Because Sample 1 is too rough to conduct the AFM test, the morphology of Sample 1 is analyzed by SEM. It is obviously seen that the surface roughness of the $CsPbBr_3$ microplates will decrease from 17.88 nm to 0.714 nm when the mass of the weight increases 0 to 13 g, suggesting a slow and suitable evaporation rate will be beneficial for the formation of $CsPbBr_3$ microplates. By comparison, the optimal evaporation rate is about 7.5 μL/h for the synthesis of $CsPbBr_3$ microplates with atom-level smooth surface.

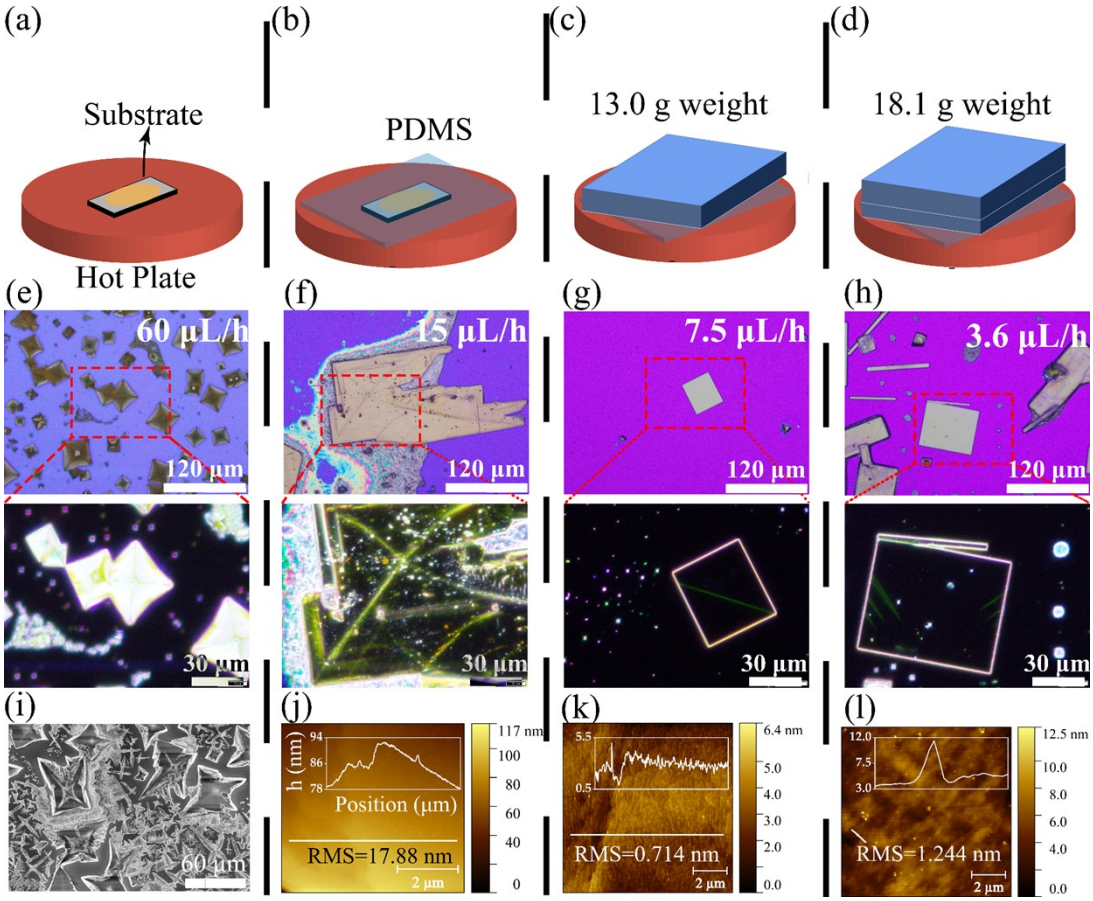

Fig. S2 (a–d) Schematic illustration of the growth process with different evaporation rates of 60, 45, 7.5, and 3.6 μL/h, respectively. (e–h) Optical images of the $CsPbBr_3$ samples with different evaporate rates. (i) The SEM image of Sample 1. (j–k) the corresponding AFM images of Samples 2-4.

3. Morphological characterization of Au nanospheres (Au NSs) with different diameters

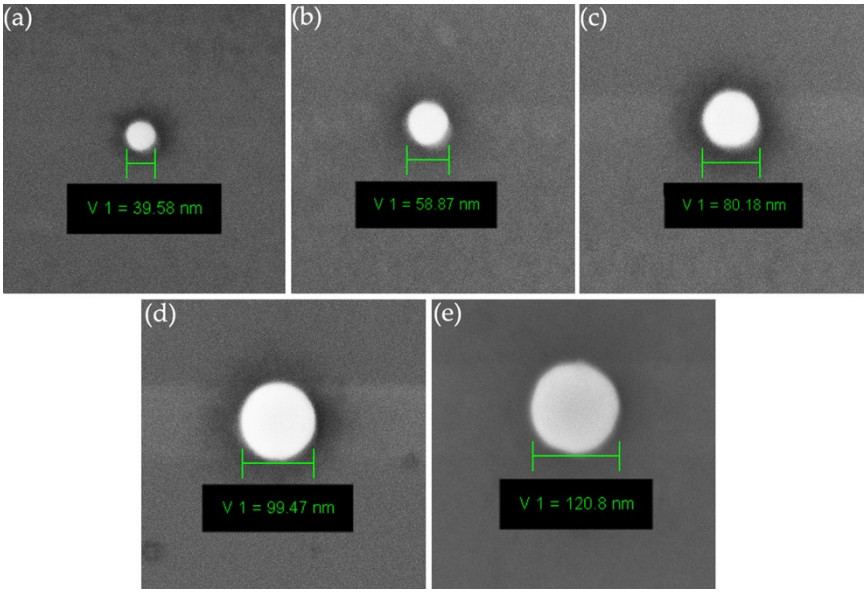

Fig. S3 The scanning electron microscope (SEM) images of the Au NSs with different diameters.

To obtain the size distribution information, the SEM image of the dispersed Au NSs with a mean diameter of 60 nm on silica substrate are displayed in Fig. S4. By measuring the diameter of 87 Au NSs, the statistic diagram of the diameter of the Au NSs are shown in the inset. According to the size distribution diagram, the average diameter of the Au NSs can be deduced to be 59.87 nm, which is in good coincident with the average diameter of 60 nm.

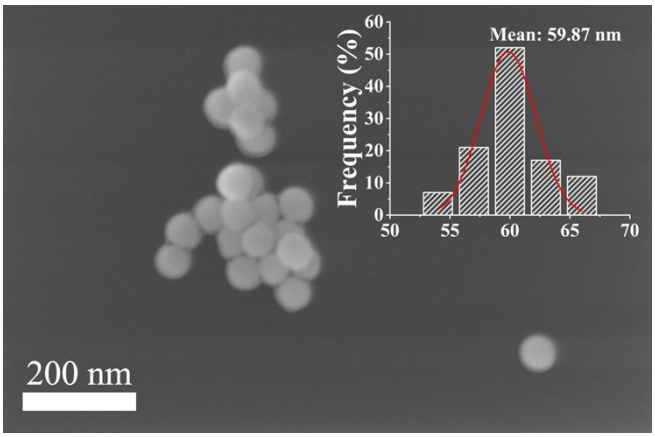

Fig. S4 The SEM image of the Au NSs with a mean diameter of 60 nm on silica substrate. And the statistic diameter of the Au NS diameter is shown in the inset.

4. Morphological characterization of $CsPbBr_3$ microplates

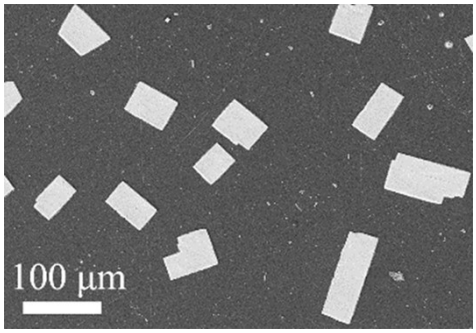

Fig. S5 Typical SEM image of the $CsPbBr_3$ microplates grown on SiO_2 substrate.

5. Optical property characterizations of $CsPbBr_3$ microplates.

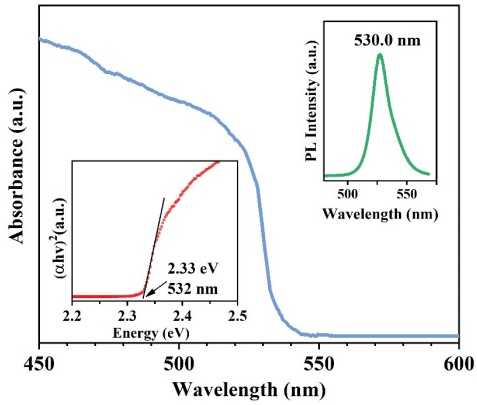

Fig. S6 Representative absorption spectrum of the $CsPbBr_3$ microplates. And the top-right inset and the lower-left give PL spectrum and the Tauc plots of the $CsPbBr_3$ microplates, respectively.

6. Crystallographic characterization of $CsPbBr_3$ microplates

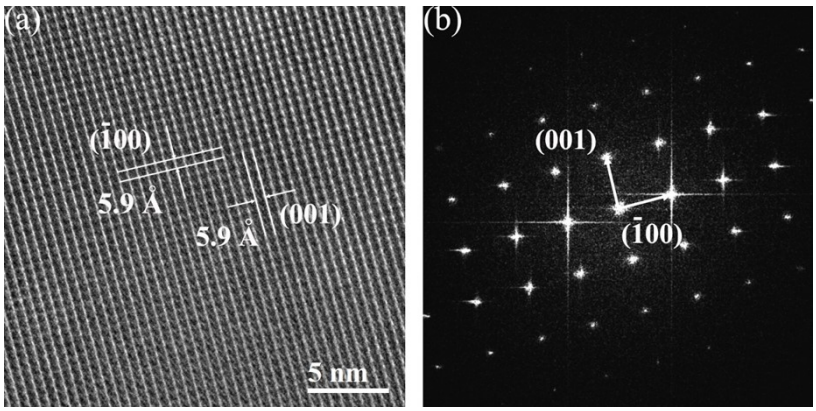

Fig. S7 (a) Representative TEM image of the $CsPbBr_3$ microplate and (b) the corresponding Fast Fourier transform (FFT) pattern.

7. Typical I–V curves of the $CsPbBr_3$ photodetectors with and without 60-nm Au NS

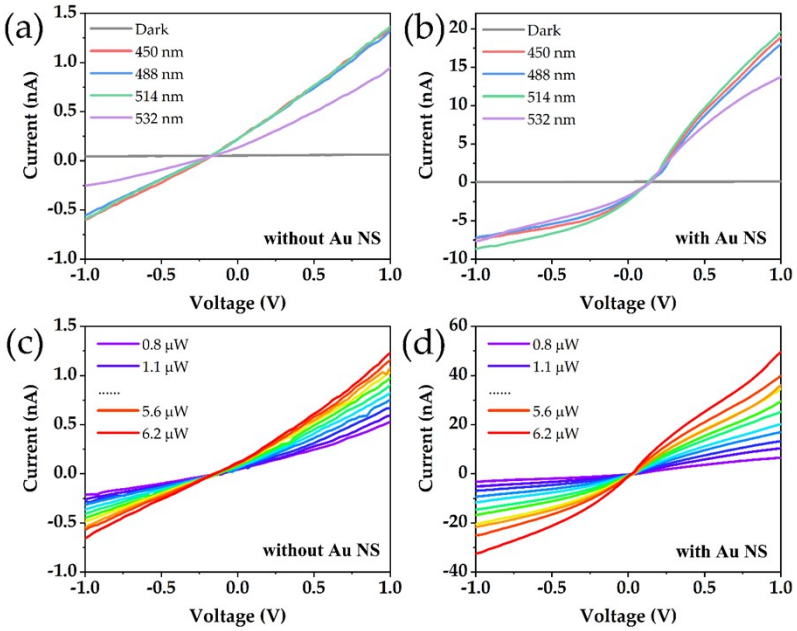

Fig. S8 Photosensitive performances of the $CsPbBr_3$ microplate with or without 60-nm Au NS. (a, b) Typical photocurrent-voltage curves of the $CsPbBr_3$ PD without or with Au NS under different irradiations with a power density of 0.482 mW/cm^2. (c, d) I-V curves of pristine $CsPbBr_3$ and $Au/CsPbBr_3$ hybrid structure under 514-nm irradiation, respectively.

8. The photosensitive behaviors of the 120-nm Au NS/$CsPbBr_3$ hybrid structure

To better comprehend the physical mechanism of the $CsPbBr_3$ PD with optical Au NSs (60 nm), Fig. S7(a) gives the typical I–V curves of the PDs with and without 120-nm Au NS under different illumination with the same power density of 0.482 mW/cm^2. In Fig. S7(c), the photocurrent enhancement factor of the hybrid structure with 120-nm Au NS is only 84.4% under the same 514-nm irradiation (P = 0.482 mW/cm^2), which is far smaller than that (1145%) of the hybrid structure with 60-nm Au NS. According to Ruffino et al. report[4], the surface work function of Au NS almost keeps unvaried with its diameter if the Au NS diameter is greater than 10 nm. Compared with 60 nm Au NS, the radiation recombination suppression of the Schottky junction in 120 nm Au NS/$CsPbBr_3$ hybrid structure should perform the same function, but both the resonance absorption and the plasmon resonance energy transfer (PRET) are weakened due to detuning with $CsPbBr_3$ excitons. It can be concluded that when the diameter of Au NS is 60 nm, the significant photocurrent enhancement factor should be mainly attributed to PRET effect.

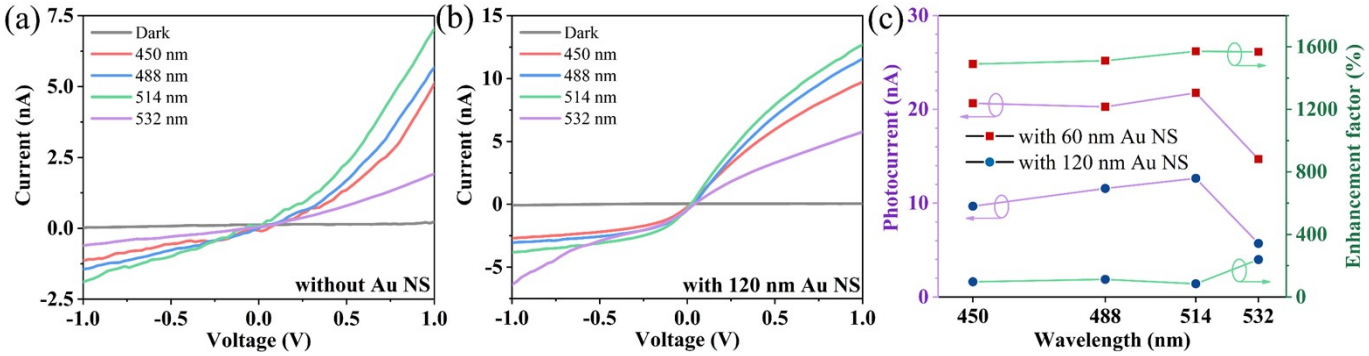

Fig. S9 (a, b) Typical photocurrent-voltage curves of the $CsPbBr_3$ PD without or with 120 nm Au NS under different irradiations with a power density of 0.482 mW/cm^2. (c) Photocurrent and the enhancement factor of $CsPbBr_3$ PDs as a function of the irradiation wavelengths at 1 V bias (P = 0.482 mW/cm^2) with 60 nm or 120 nm Au NS.

Supplementary References:

[1] M. Liao, M. Xia, Y. Xu, P. Lu and G. Niu, *Chem. Commun.*, 2023, **59**, 8758-8768.
[2] C. Møller, *Mat Fys. Medd. Dan Vid Selsk.*, 1959, **32**.
[3] C. Liu, Y. B. Cheng and Z. Ge, *Chem. Soc. Rev.*, 2020, **49**, 1653-1687.
[4] F. Ruffino, M. G. Grimaldi, F. Giannazzo, F. Roccaforte and V. Raineri, *Appl. Phys. Lett.*, 2006, **89**, 243113.